Updates on Nucleon Form Factors from Clover-on-HISQ Formulation

Yong-Chull Jang

Physics Department, Brookhaven National Laboratory

(PNDME Collaboration)

T. Bhattacharya, R. Gupta, B. Yoon (LANL), H.W Lin (MSU)

The 36th International Symposium on Lattice Field Theory,
23–28 July, 2018

East Lansing, MI, USA

HISQ Ensembles $N_f = 2+1+1$

Ensemble ID	a (fm)	$M_\pi^{\rm sea}$ (MeV)	$M_\pi^{\rm val}$ (MeV)	$L^3 \times T$	$M_\pi^{\rm val} L$	τ/a	$N_{\rm conf}$	$N_{\rm meas}^{\rm HP}$	$N_{\rm meas}^{\rm LP}$
a15m310	0.1510(20)	306.9(5)	320(5)	$16^3 \times 48$	3.93	$\{5,6,7,8,9\}$	1917	7668	122,688
$a12m310$	0.1207(11)	305.3(4)	310.2(2.8)	$24^3 \times 64$	4.55	$\{8,10,12\}$	1013	8104	64,832
a12m220S	0.1202(12)	218.1(4)	225.0(2.3)	$24^3 \times 64$	3.29	$\{8,10,12\}$	946	3784	60,544
a12m220	0.1184(10)	216.9(2)	227.9(1.9)	$32^3 \times 64$	4.38	$\{8,10,12\}$	744	2976	47,616
a12m220L	0.1189(09)	217.0(2)	227.6(1.7)	$40^3 \times 64$	5.49	$\{8,10,12,14\}$	1000	4000	128,000
a09m310	0.0888(08)	312.7(6)	313.0(2.8)	$32^3 \times 96$	4.51	$\{10,12,14,16\}$	2263	9052	144,832
a09m220	0.0872(07)	220.3(2)	225.9(1.8)	$48^3 \times 96$	4.79	$\{10,12,14,16\}$	964	7712	123,392
$a09m130$	0.0871(06)	128.2(1)	138.1(1.0)	$64^3 \times 96$	3.90	$\{10,12,14\}$	883	7064	84,768
a09m130W						$\{8,10,12,14,16\}$	1290	5160	165,120
$a06m310$	0.0582(04)	319.3(5)	319.6(2.2)	$48^3 \times 144$	4.52	$\{16,20,22,24\}$	1000	8000	64,000
a06m310W						$\{18,20,22,24\}$	500	2000	64,000
$a06m220$	0.0578(04)	229.2(4)	235.2(1.7)	$64^3 \times 144$	4.41	$\{16,20,22,24\}$	650	2600	41,600
a06m220W						$\{18,20,22,24\}$	649	2596	41,536
a06m135	0.0570(01)	135.5(2)	135.6(1.4)	$96^3 \times 192$	3.7	$\{16,18,20,22\}$	675	2700	43,200

- 4th lattice spacing $a \approx 0.15\,\mathrm{fm}$ and different smearing with larger gaussian width W
- different volumes for the form factor analysis
- Truncated solver bias correction for all τ/a
  $\rightarrow$ All but the $a09m130$ at $Q^2 \neq 0$ are bias corrected.
- Statistics are increased.

Correlator Fits: 2-pt

- We use 4-state fits for 2-point correlator.

$$C^{2\mathrm{pt}}(t, \boldsymbol{p}) = |\mathcal{A}_0|^2 e^{-E_0 t} + |\mathcal{A}_1|^2 e^{-E_1 t} + |\mathcal{A}_2|^2 e^{-E_2 t} + |\mathcal{A}_3|^2 e^{-E_3 t} + \cdots$$

- plot effective mass from fits and data

$$E_{\mathrm{eff}}(t) = \log \frac{C^{2\mathrm{pt}}(t)}{C^{2\mathrm{pt}}(t+1)}$$

- The lowest three states are used in the 3-point correlator fits to extract the form factors.

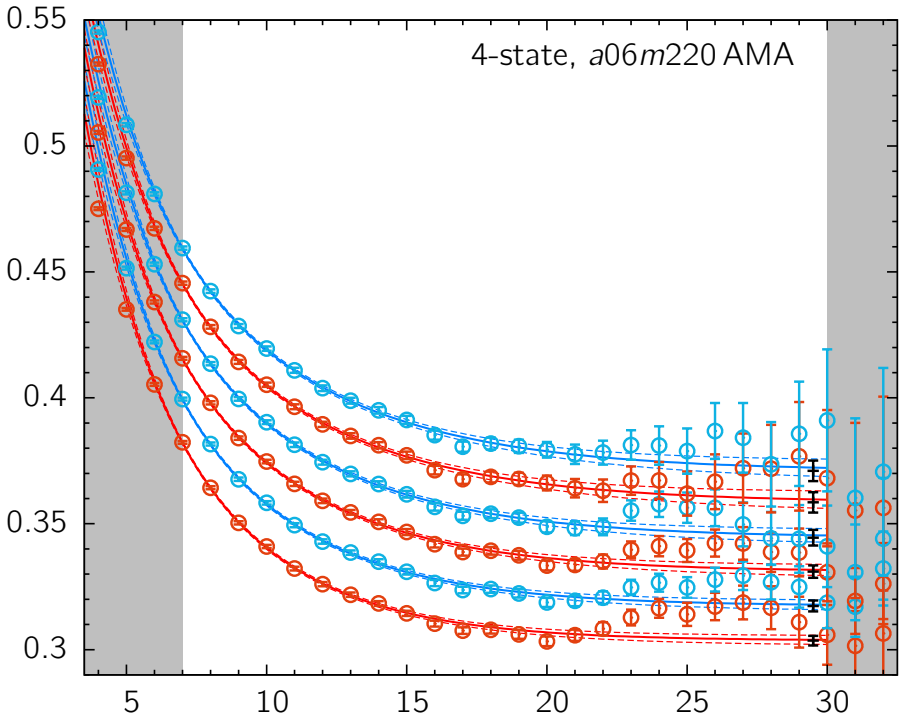

Nucleon Electromagnetic Form Factors

Form Factor Decomposition

- Isovector EM form factors, charge, magnetic moment, charge radii

$$\langle N(\vec{p}_f)|V_\mu(\vec{q})|N(\vec{p}_i)\rangle = \overline{u}(\vec{p}_f)\left[F_1(Q^2)\gamma_\mu + \sigma_{\mu\nu}q_\nu\frac{F_2(Q^2)}{2M}\right]u(\vec{p}_i)$$

$$q = p_f - p_i,\ Q^2 = -q^2 = \vec{p}_f^{\,2} - (E-M)^2,\ \vec{p}_i = 0$$

$$G_E(Q^2) = F_1(Q^2) - \frac{Q^2}{4M^2}F_2(Q^2) \rightarrow \langle r_E^2\rangle,\ G_E(0) \equiv g_V$$

$$G_M(Q^2) = F_1(Q^2) + F_2(Q^2) \qquad \rightarrow \langle r_M^2\rangle,\ G_M(0)/G_E(0) \equiv \mu$$

$$\langle r_{E,M}^2\rangle = -6\frac{d}{dQ^2}\left(\frac{G_{E,M}(Q^2)}{G_{E,M}(0)}\right)\Bigg|_{Q^2=0}$$

$$\mu = 1 + \kappa, \quad (\mu = \mu^p - \mu^n, \kappa = \kappa^p - \kappa^n)$$

Vector Form Factors $G_E(Q^2), G_M(Q^2)$

- Matrix elements $\langle m'|\mathcal{O}_\Gamma|n\rangle$ are extracted from a simultaneous fit to the correlator $C_\Gamma^{(3pt)}$ calculated at multiple τ.

$$
\begin{aligned}
C_\Gamma^{(3pt)}(t;\tau;\boldsymbol{p}',\boldsymbol{p}=\boldsymbol{0}) = {} & |\mathcal{A}_0'||\mathcal{A}_0|\langle 0'|\mathcal{O}_\Gamma|0\rangle e^{-E_0 t - M_0(\tau-t)} \\
& + |\mathcal{A}_1'||\mathcal{A}_1|\langle 1'|\mathcal{O}_\Gamma|1\rangle e^{-E_1 t - M_1(\tau-t)} + |\mathcal{A}_2'||\mathcal{A}_2|\langle 2'|\mathcal{O}_\Gamma|2\rangle e^{-E_2 t - M_2(\tau-t)} \\
& + |\mathcal{A}_0'||\mathcal{A}_1|\langle 0'|\mathcal{O}_\Gamma|1\rangle e^{-E_0 t - M_1(\tau-t)} + |\mathcal{A}_1'||\mathcal{A}_0|\langle 1'|\mathcal{O}_\Gamma|0\rangle e^{-E_1 t - M_0(\tau-t)} \\
& + |\mathcal{A}_0'||\mathcal{A}_2|\langle 0'|\mathcal{O}_\Gamma|2\rangle e^{-E_0 t - M_2(\tau-t)} + |\mathcal{A}_2'||\mathcal{A}_0|\langle 2'|\mathcal{O}_\Gamma|0\rangle e^{-E_2 t - M_0(\tau-t)} \\
& + |\mathcal{A}_1'||\mathcal{A}_2|\langle 1'|\mathcal{O}_\Gamma|2\rangle e^{-E_1 t - M_2(\tau-t)} + |\mathcal{A}_2'||\mathcal{A}_1|\langle 2'|\mathcal{O}_\Gamma|1\rangle e^{-E_2 t - M_1(\tau-t)}
\end{aligned}
$$

$$
\begin{aligned}
C^{2pt}(t,\boldsymbol{p}) &= |\mathcal{A}_0'|^2 e^{-E_0 t} + |\mathcal{A}_1'|^2 e^{-E_1 t} + |\mathcal{A}_2'|^2 e^{-E_2 t} + |\mathcal{A}_3'|^2 e^{-E_3 t} + \cdots \\
&: \boldsymbol{p} = \boldsymbol{0} \rightarrow \mathcal{A}_i' = \mathcal{A}_i, E_i = M_i
\end{aligned}
$$

- Data is displayed using the following ratio.

$$
\mathcal{R}_\Gamma(t,\tau,\boldsymbol{p}',\boldsymbol{p}) = \frac{C_\Gamma^{(3pt)}(t,\tau;\boldsymbol{p}',\boldsymbol{p})}{C^{(2pt)}(\tau,\boldsymbol{p})} \times \left[\frac{C^{(2pt)}(t,\boldsymbol{p})C^{(2pt)}(\tau,\boldsymbol{p})C^{(2pt)}(\tau-t,\boldsymbol{p}')}{C^{(2pt)}(t,\boldsymbol{p}')C^{(2pt)}(\tau,\boldsymbol{p}')C^{(2pt)}(\tau-t,\boldsymbol{p})}\right]^{1/2} \xrightarrow[0 \ll t,\tau-t]{\tau\to\infty} \langle 0'|\mathcal{O}_\Gamma|0\rangle
$$

average over γ_1, γ_2, γ_3

Γ	γ_1	γ_2	γ_3	γ_4
Re	$-q_2 G_M$	$q_1 G_M$		$(M+E)G_E$
Im	$q_1 G_E$	$q_2 G_E$	$q_3 G_E$	

Controlling Excited State Contribution to G_E

We use $\mathrm{Re}\,V_4$ to extract G_E.

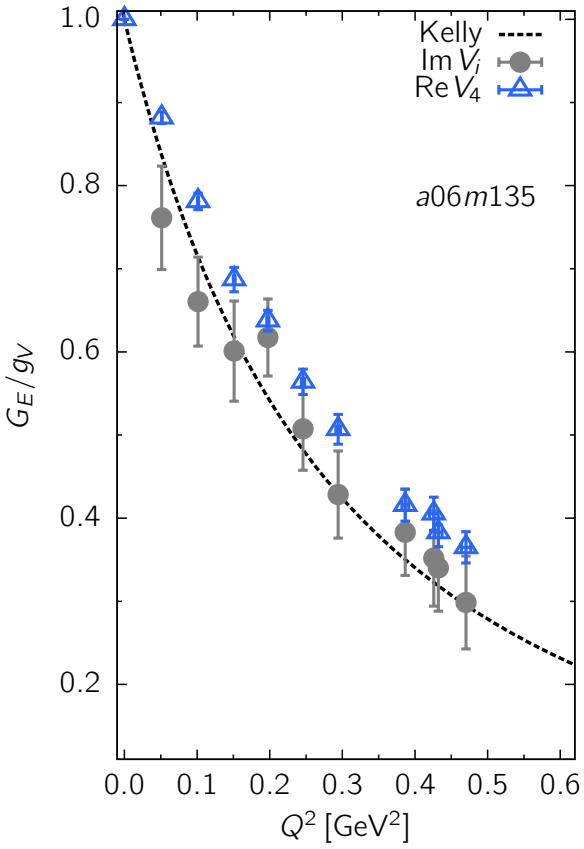

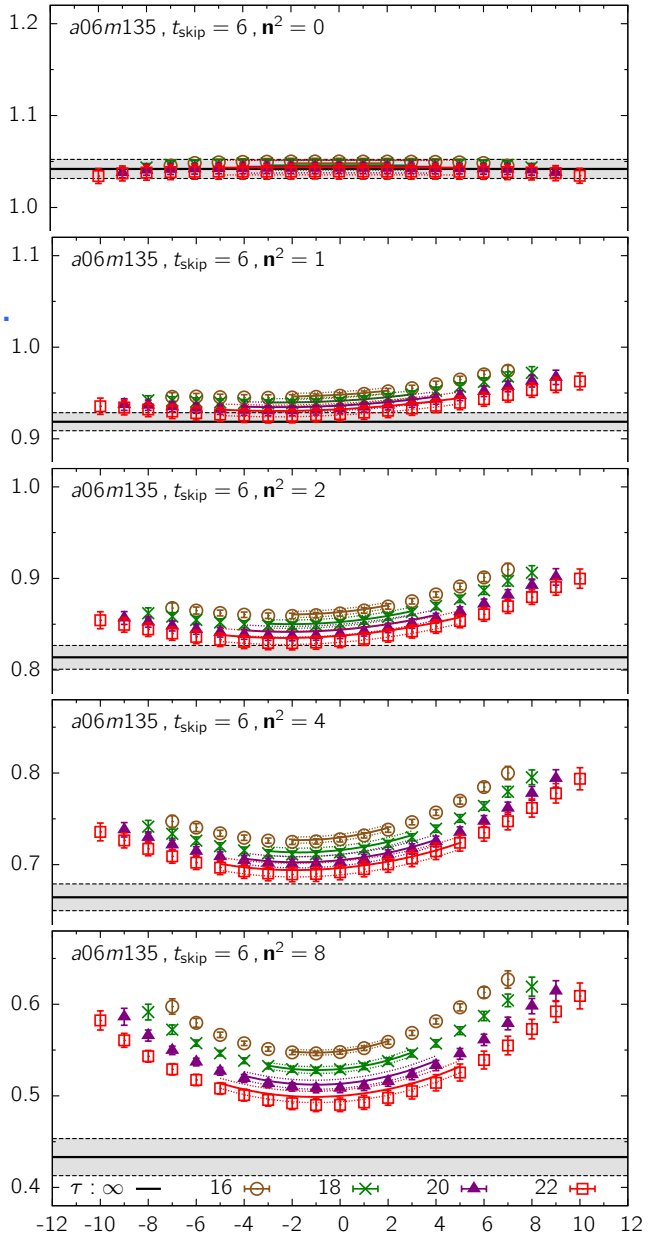

$\mathrm{Re}\,\mathcal{R}_4 \to G_E(Q^2)$

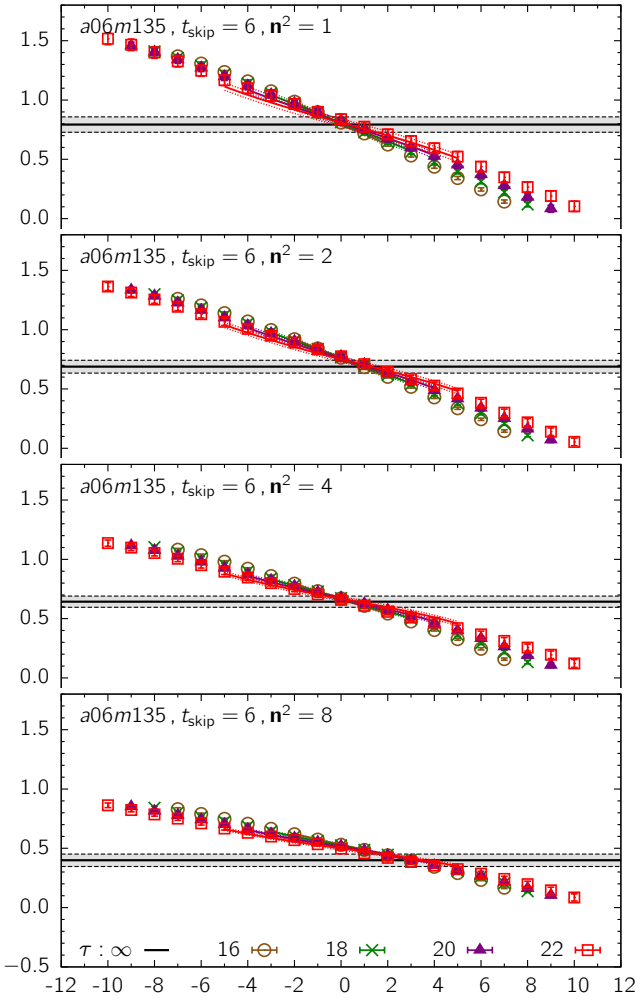

$\mathrm{Im}\,\mathcal{R}_i \to G_E(Q^2)$

Controlling Excited State Contribution to G_M

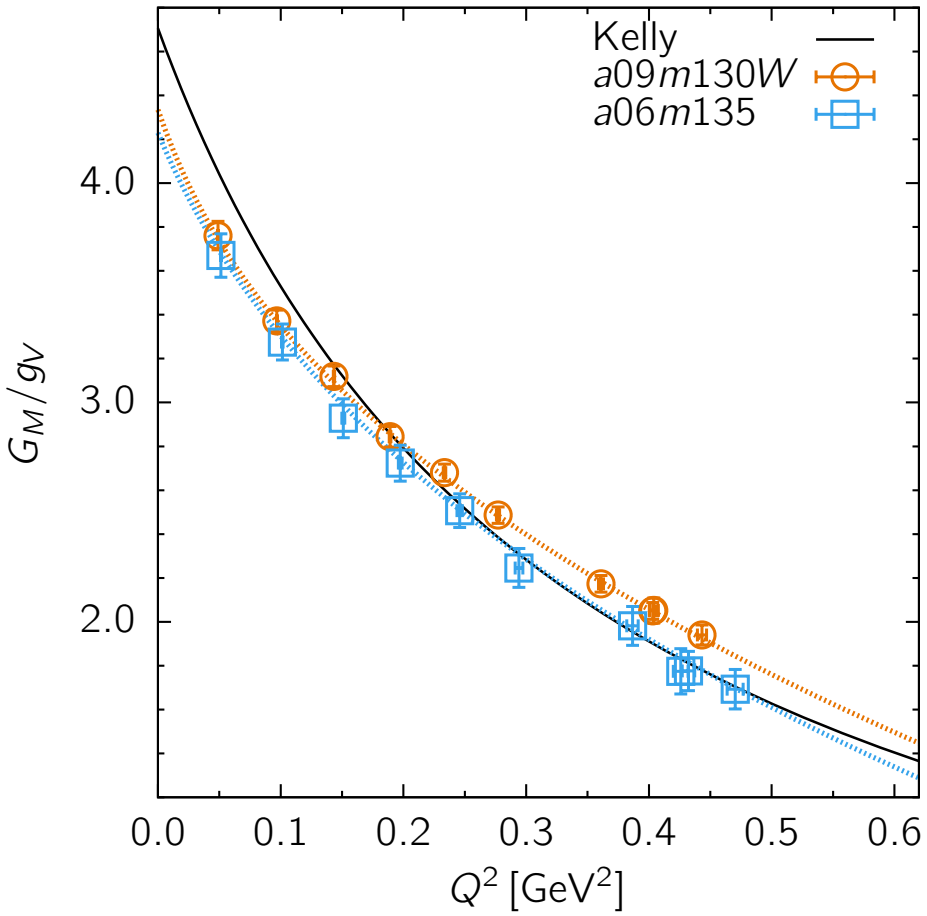

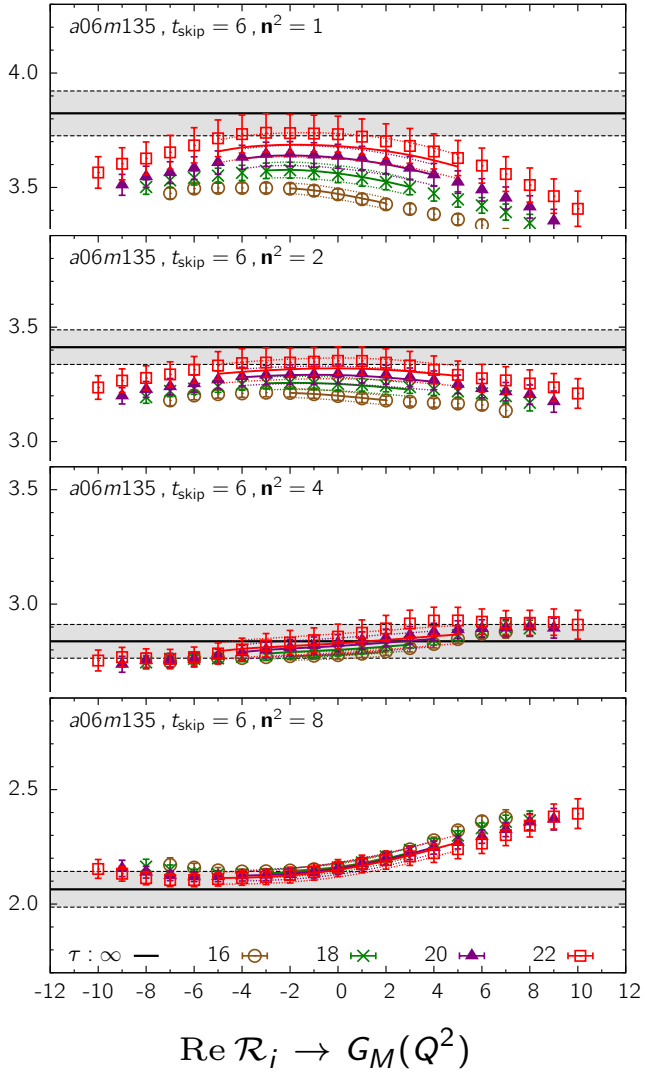

Q^2 Fits to Electromagnetic Form Factors

- dipole

$$G_E(Q^2) = \frac{G_E(0)}{(1+Q^2/\mathcal{M}_E^2)^2} \quad \Longrightarrow \quad \langle r_E^2 \rangle = \frac{12}{\mathcal{M}_E^2}$$

- z-expansion w/o sumrule constraints

$$\frac{G_E(Q^2)}{G_E(0)} = \sum_{k=0}^{\infty} a_k z(Q^2)^k \,, \quad z = \frac{\sqrt{t_{\rm cut}+Q^2} - \sqrt{t_{\rm cut}+\bar{t}_0}}{\sqrt{t_{\rm cut}+Q^2} + \sqrt{t_{\rm cut}+\bar{t}_0}} \,, \quad (t_{\rm cut} = 4M_\pi^2)$$

$$\sum_{k=n}^{k_{\rm max}} k(k-1)\ldots(k-n+1)a_k = 0 \qquad n = 0,1,2,3\,.$$

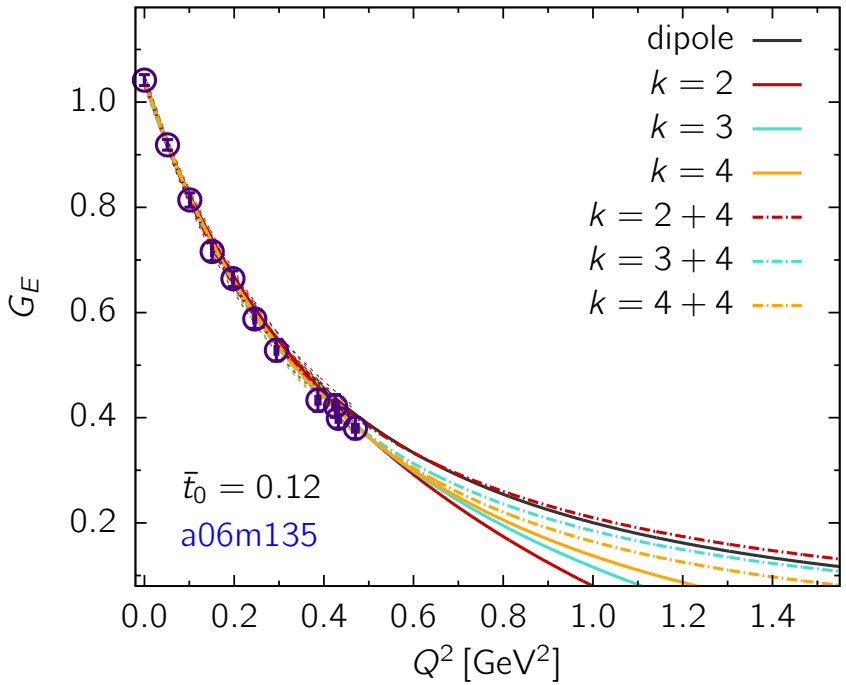

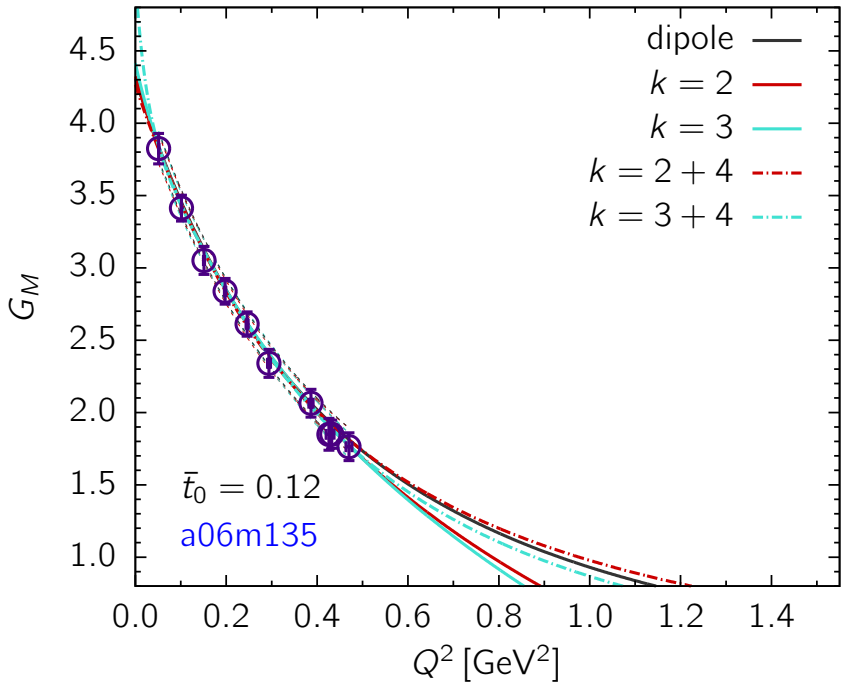

Electric Form Factors $G_E(Q^2)$ and Charge Radius $\langle r_E^2 \rangle$

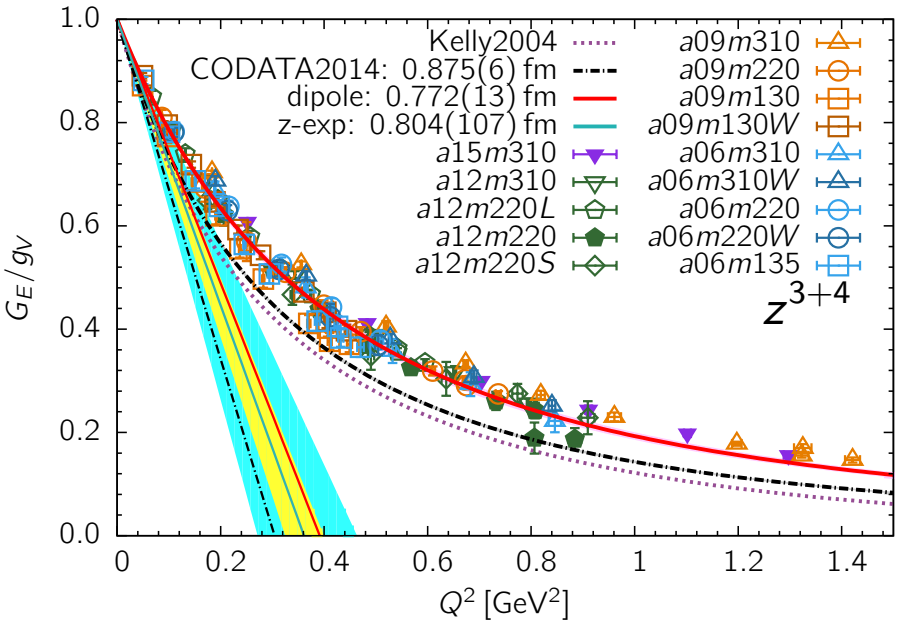

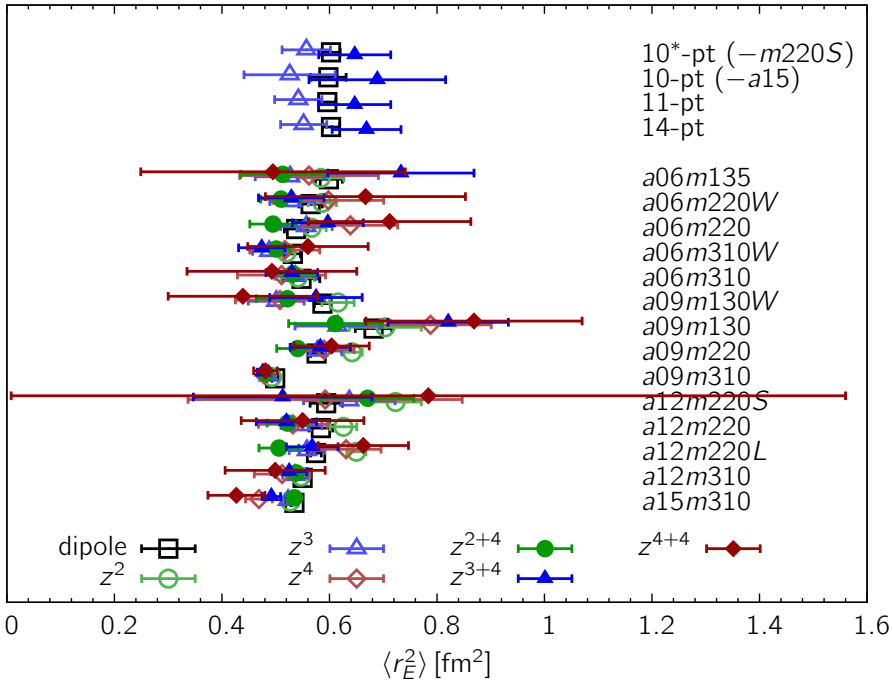

- central value: 11-point extrapolation $\langle r_E^2 \rangle(a, M_\pi, M_\pi L)$
- systematic error: difference of r_E from two physical ensembles
- $r_E = 0.804(42)(98)\,\mathrm{fm}$ from z-expansion fit @ z^{3+4}
- $r_E = 0.772(10)(8)\,\mathrm{fm}$ from dipole fit
- $r_E = 0.875(6)\,\mathrm{fm}$ (CODATA-2014, electron) [Rev. Mod. Phys. 88, 035009 (2016)]
- $r_E = 0.8409(4)\,\mathrm{fm}$ (Lamb shift in muonic hydrogen) [EPJ Web Conf. 113,01006 (2016)]

Electric Charge Radius $\langle r_E^2 \rangle$: dipole versus z^{3+4}

$$\langle r_E^2 \rangle = c_1^E + c_2^E a + c_3^E \ln(M_\pi^2/M_\rho^2) + c_4^E \ln(M_\pi^2/M_\rho^2) e^{-M_\pi L}$$

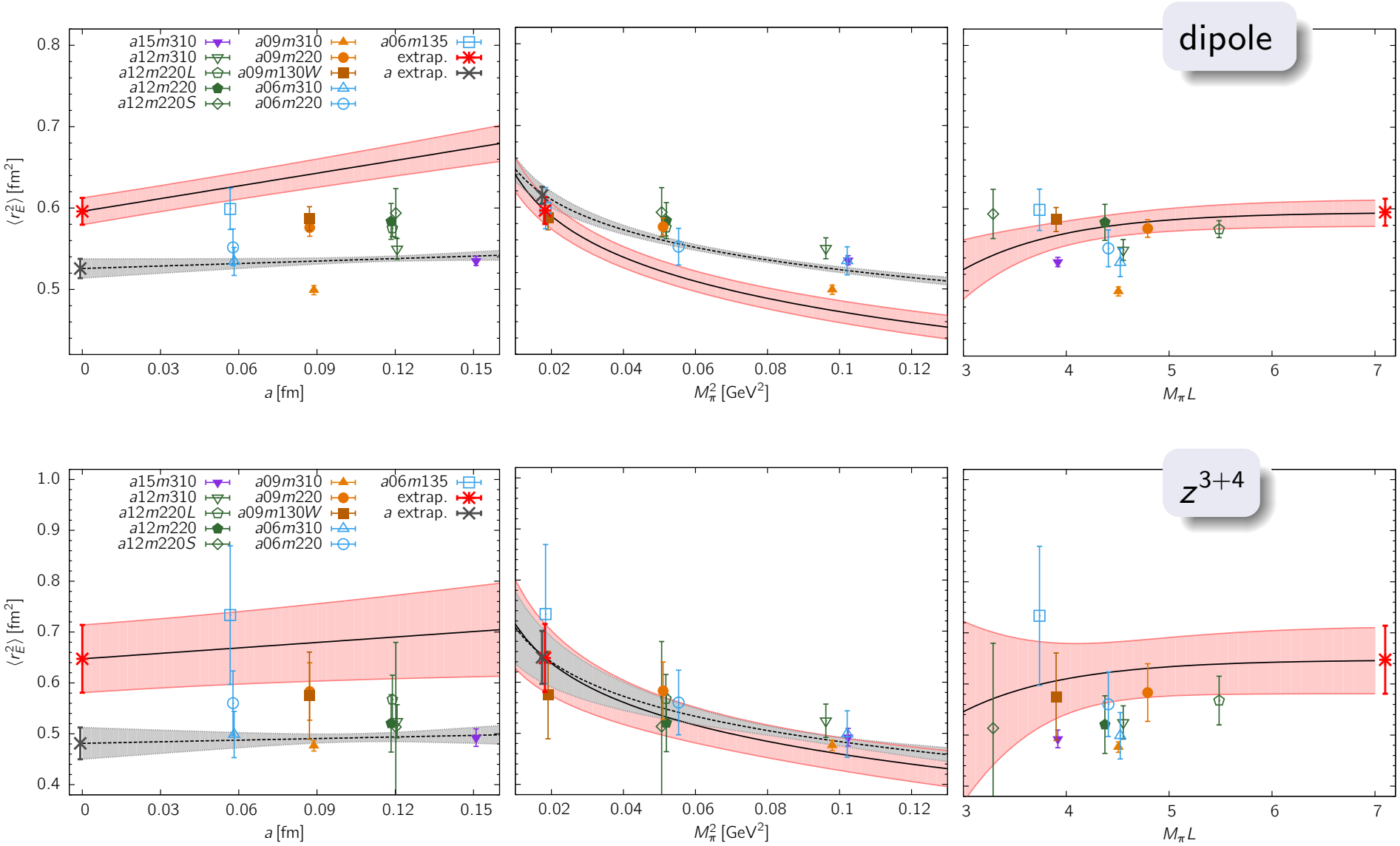

Magnetic Form Factors $G_M(Q^2)$ and Charge Radius $\langle r_M^2 \rangle$

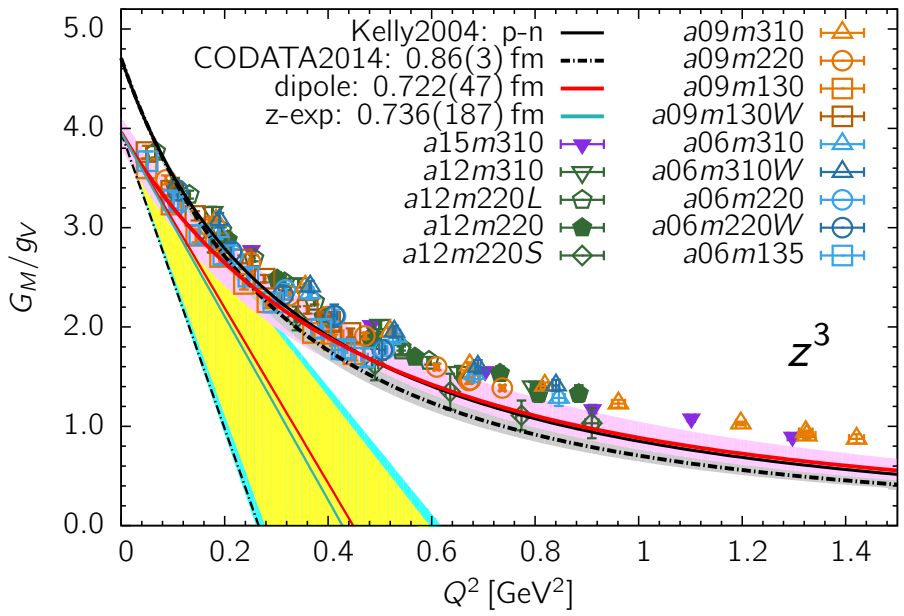

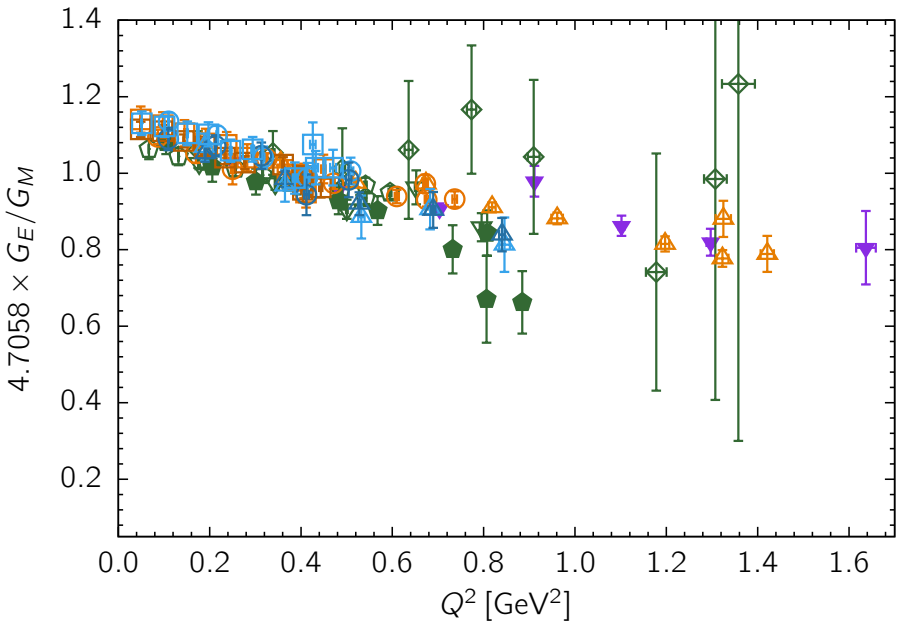

- central value: 11-point extrapolation $\langle r_M^2 \rangle(a, M_\pi, M_\pi L)$, $\langle \mu \rangle(a, M_\pi, M_\pi L)$
- systematic error: difference of $\langle r_M^2 \rangle$ from two physical ensembles
  and of deviation from the average of $a \approx 0.06\,\mathrm{fm}$ results of $\langle \mu \rangle$
- $r_M = 0.736(166)(86)\,\mathrm{fm}$, $\mu = 3.99(32)(17)$ from z-expansion fit @ z^3
- $r_M = 0.722(23)(41)\,\mathrm{fm}$, $\mu = 3.96(10)(12)$ from dipole fit
- $r_M = 0.86(3)\,\mathrm{fm}$ (CODATA-2014, electron) [Rev. Mod. Phys. 88, 035009 (2016)], $\mu = 4.7058$ [PDG]
- To compare the slope at $G_M(Q^2 = 0)$, different μ are shifted to the common point μ @ dipole.
- μ from dipole and z^3 fits are 15% smaller than the experimental value. G_E/G_M data shows this difference. The difference does not come from a fit instability of G_M.

Magnetic Charge Radius $\langle r_M^2 \rangle$: dipole versus z^3

$$\langle r_M^2 \rangle = c_1^M + c_2^M a + c_3^M / M_\pi + (c_4^M / M_\pi) e^{-M_\pi L}$$

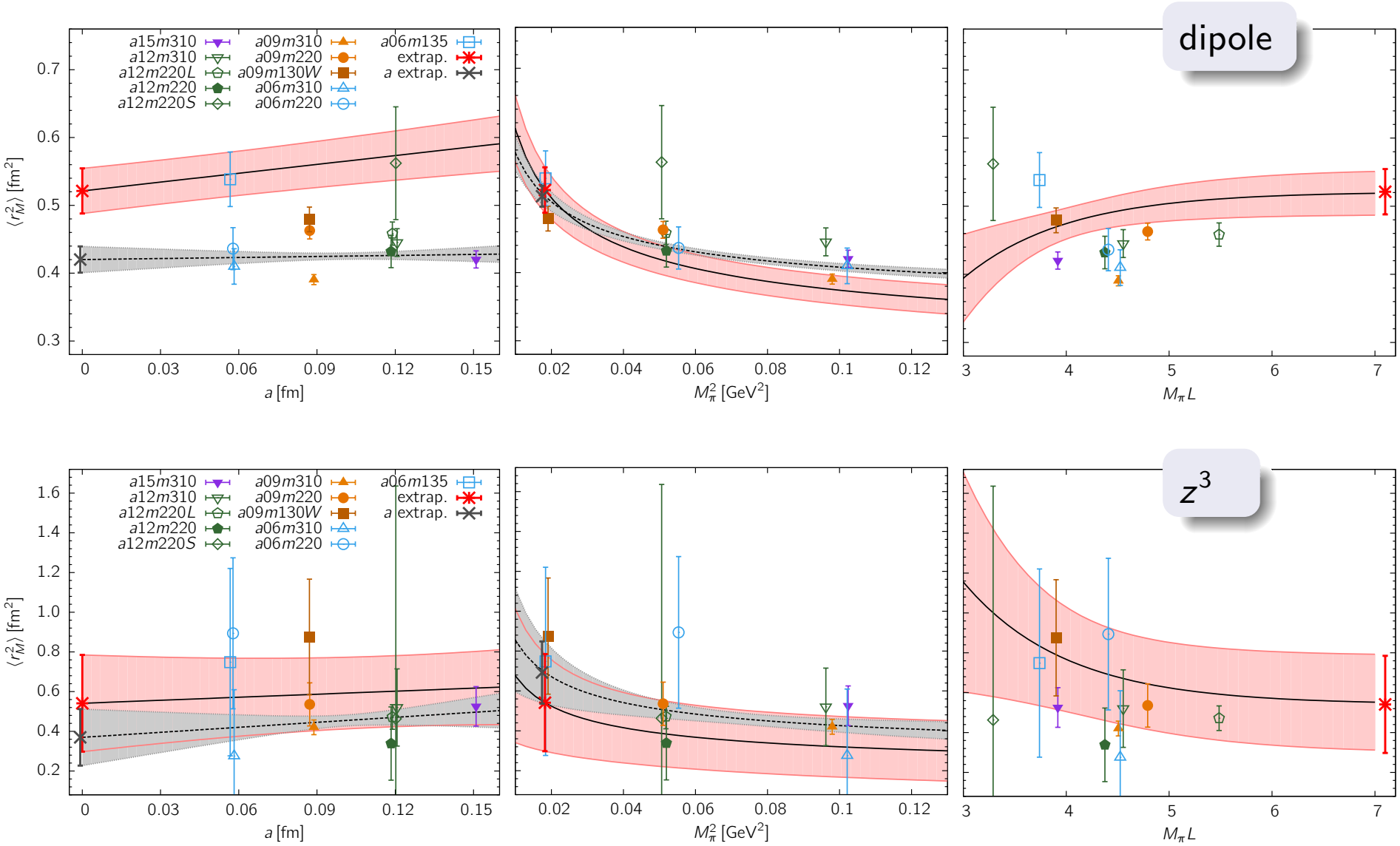

Magnetic Moment $\mu_p - \mu_n$: dipole versus z^3

$$\langle \mu \rangle = c_1^\mu + c_2^\mu a + c_3^\mu M_\pi + c_4^\mu M_\pi \left(1 - \frac{2}{M_\pi L}\right) e^{-M_\pi L}$$

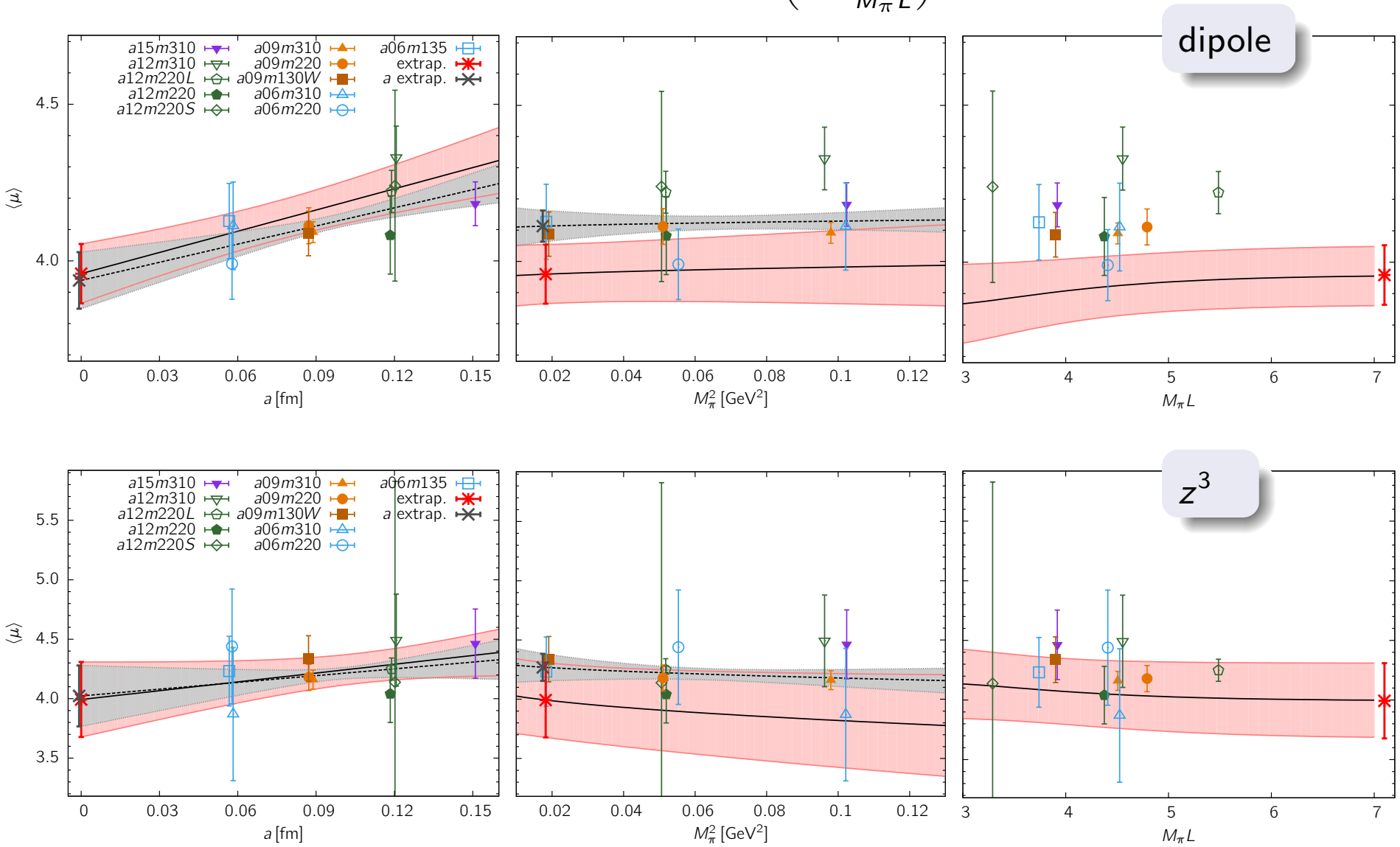

Nucleon Axial Form Factors

Form Factor Decomposition

- Isovector axial form factors, charge, charge radius

$$\langle N(\vec{p}_f)|A_\mu(\vec{Q})|N(\vec{p}_i)\rangle = \overline{u}(\vec{p}_f)\left[G_A(Q^2)\gamma_\mu + q_\mu \frac{\widetilde{G}_P(Q^2)}{2M}\right]\gamma_5 u(\vec{p}_i)$$

$$\langle N(\vec{p}_f)|P_\mu(\vec{q})|N(\vec{p}_i)\rangle = \overline{u}(\vec{p}_f)\left[G_P(Q^2)\gamma_5\right]u(\vec{p}_i)$$

$$q = p_f - p_i,\ Q^2 = -q^2 = \vec{p}_f^{\,2} - (E-M)^2,\ \vec{p}_i = 0$$

$$\langle r_A^2\rangle = -6\frac{d}{dQ^2}\left(\frac{G_A(Q^2)}{G_A(0)}\right)\Bigg|_{Q^2=0},\ G_A(0) \equiv g_A$$

Axial Form Factors $G_A(Q^2)$, $\widetilde{G}_P(Q^2)$, $G_P(Q^2)$

- Matrix elements $\langle m'|\mathcal{O}_\Gamma|n\rangle$ are extracted from a simultaneous fit to the correlator $C_\Gamma^{(3pt)}$ calculated at multiple τ.

$$
\begin{aligned}
C_\Gamma^{(3pt)}(t;\tau;\boldsymbol{p}',\boldsymbol{p}=\boldsymbol{0}) = {} & |\mathcal{A}_0'||\mathcal{A}_0|\langle 0'|\mathcal{O}_\Gamma|0\rangle e^{-E_0 t - M_0(\tau-t)} \\
& + |\mathcal{A}_1'||\mathcal{A}_1|\langle 1'|\mathcal{O}_\Gamma|1\rangle e^{-E_1 t - M_1(\tau-t)} + |\mathcal{A}_2'||\mathcal{A}_2|\langle 2'|\mathcal{O}_\Gamma|2\rangle e^{-E_2 t - M_2(\tau-t)} \\
& + |\mathcal{A}_0'||\mathcal{A}_1|\langle 0'|\mathcal{O}_\Gamma|1\rangle e^{-E_0 t - M_1(\tau-t)} + |\mathcal{A}_1'||\mathcal{A}_0|\langle 1'|\mathcal{O}_\Gamma|0\rangle e^{-E_1 t - M_0(\tau-t)} \\
& + |\mathcal{A}_0'||\mathcal{A}_2|\langle 0'|\mathcal{O}_\Gamma|2\rangle e^{-E_0 t - M_2(\tau-t)} + |\mathcal{A}_2'||\mathcal{A}_0|\langle 2'|\mathcal{O}_\Gamma|0\rangle e^{-E_2 t - M_0(\tau-t)} \\
& + |\mathcal{A}_1'||\mathcal{A}_2|\langle 1'|\mathcal{O}_\Gamma|2\rangle e^{-E_1 t - M_2(\tau-t)} + |\mathcal{A}_2'||\mathcal{A}_1|\langle 2'|\mathcal{O}_\Gamma|1\rangle e^{-E_2 t - M_1(\tau-t)}
\end{aligned}
$$

$$
\begin{aligned}
C^{2pt}(t,\boldsymbol{p}) &= |\mathcal{A}_0'|^2 e^{-E_0 t} + |\mathcal{A}_1'|^2 e^{-E_1 t} + |\mathcal{A}_2'|^2 e^{-E_2 t} + |\mathcal{A}_3'|^2 e^{-E_3 t} + \cdots \\
&: \boldsymbol{p} = \boldsymbol{0} \rightarrow \mathcal{A}_i' = \mathcal{A}_i, E_i = M_i
\end{aligned}
$$

- Data is displayed using the following ratio.

$$
\mathcal{R}_\Gamma(t,\tau,\boldsymbol{p}',\boldsymbol{p}) = \frac{C_\Gamma^{(3pt)}(t,\tau;\boldsymbol{p}',\boldsymbol{p})}{C^{(2pt)}(\tau,\boldsymbol{p})} \times \left[\frac{C^{(2pt)}(t,\boldsymbol{p})C^{(2pt)}(\tau,\boldsymbol{p})C^{(2pt)}(\tau-t,\boldsymbol{p}')}{C^{(2pt)}(t,\boldsymbol{p}')C^{(2pt)}(\tau,\boldsymbol{p}')C^{(2pt)}(\tau-t,\boldsymbol{p})}\right]^{1/2} \xrightarrow[0 \ll t,\tau-t]{\tau\to\infty} \langle 0'|\mathcal{O}_\Gamma|0\rangle
$$

Γ	$\gamma_5\gamma_1$	$\gamma_5\gamma_2$	$\gamma_5\gamma_3$	$\gamma_5\gamma_4$	γ_5
Re				$q_3\{(M-E)\widetilde{G}_P + 2MG_A\}$	$q_3 G_P$
Im	$q_1 q_3 \widetilde{G}_P$	$-q_2 q_3 \widetilde{G}_P$	$-q_3^2\widetilde{G}_P + 2M(M+E)G_A$		

Controlling Excited State Contribution to G_A, $\widetilde{G}_P$, G_P

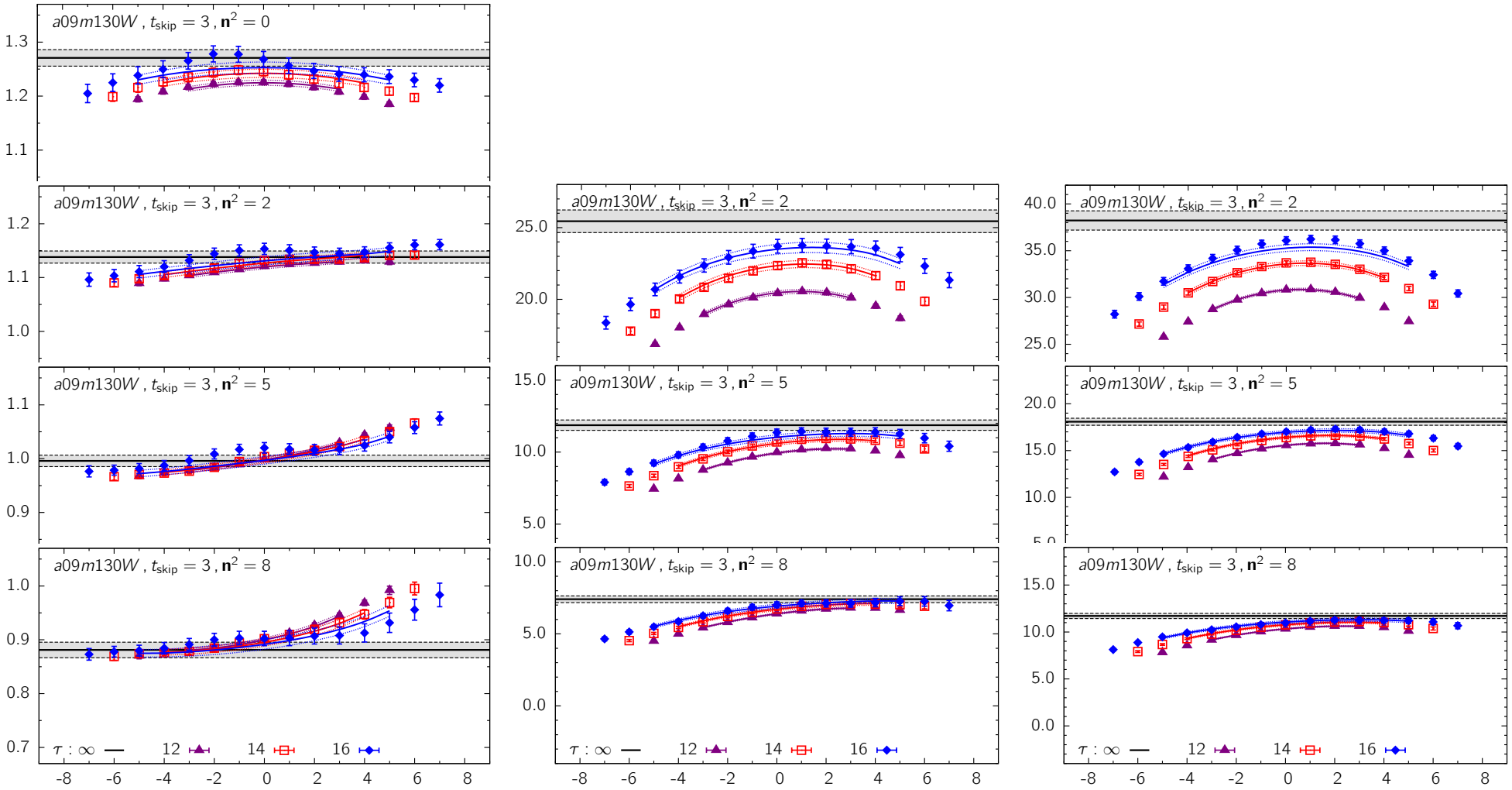

$\mathrm{Im}\,\mathcal{R}_{53}, q_3 = 0 \to G_A(Q^2)$ $\mathrm{Im}\,\mathcal{R}_{51} \to \widetilde{G}_P(Q^2)$ $\mathrm{Re}\,\mathcal{R}_5 \to G_P(Q^2)$

Very similar Excited State Contamination in $\widetilde{G}_P$ and G_P

Fitting Q^2 dependence of the Axial Form Factor

- dipole

$$G_A(Q^2) = \frac{G_A(0)}{(1+Q^2/\mathcal{M}_A^2)^2} \quad \Longrightarrow \quad \langle r_A^2 \rangle = \frac{12}{\mathcal{M}_A^2}$$

- z-expansion w/o sumrule constraints $Q^n G_A(Q^2) \to 0$

$$\frac{G_A(Q^2)}{G_A(0)} = \sum_{k=0}^{\infty} a_k z(Q^2)^k \,, \quad z = \frac{\sqrt{t_{\rm cut}+Q^2} - \sqrt{t_{\rm cut}+\bar{t}_0}}{\sqrt{t_{\rm cut}+Q^2} + \sqrt{t_{\rm cut}+\bar{t}_0}} \,, \quad (t_{\rm cut} = 9M_\pi^2)$$

$$\sum_{k=n}^{k_{\rm max}} k(k-1)\ldots(k-n+1)a_k = 0 \qquad n = 0,1,2,3\,.$$

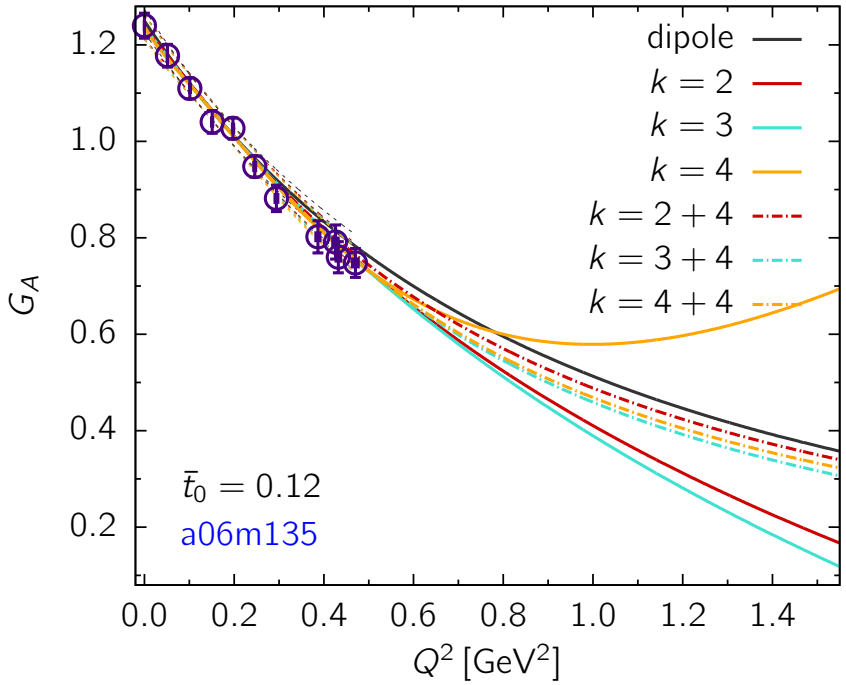

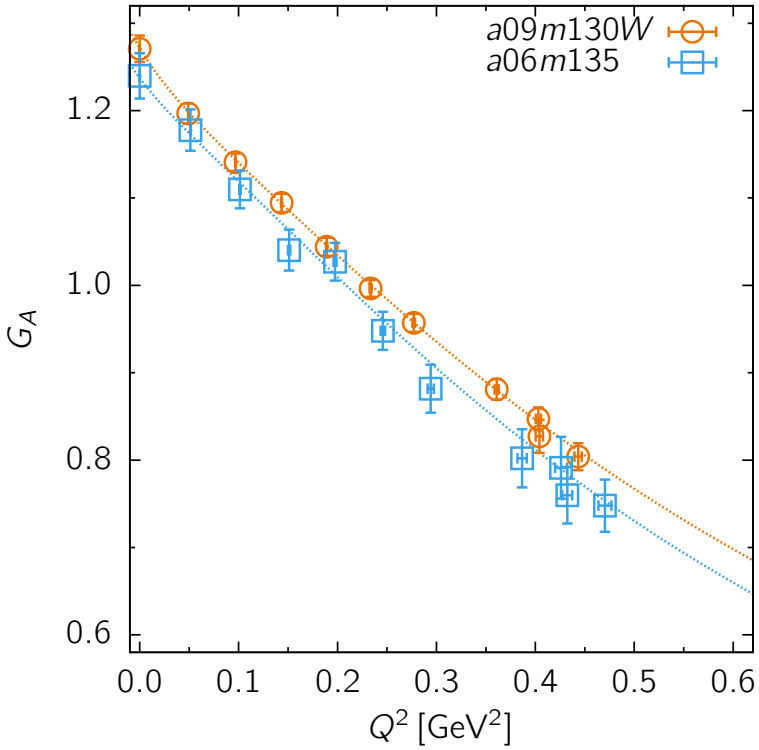

Axial Form Factor $G_A(Q^2)$ and Charge Radius $\langle r_A^2 \rangle$

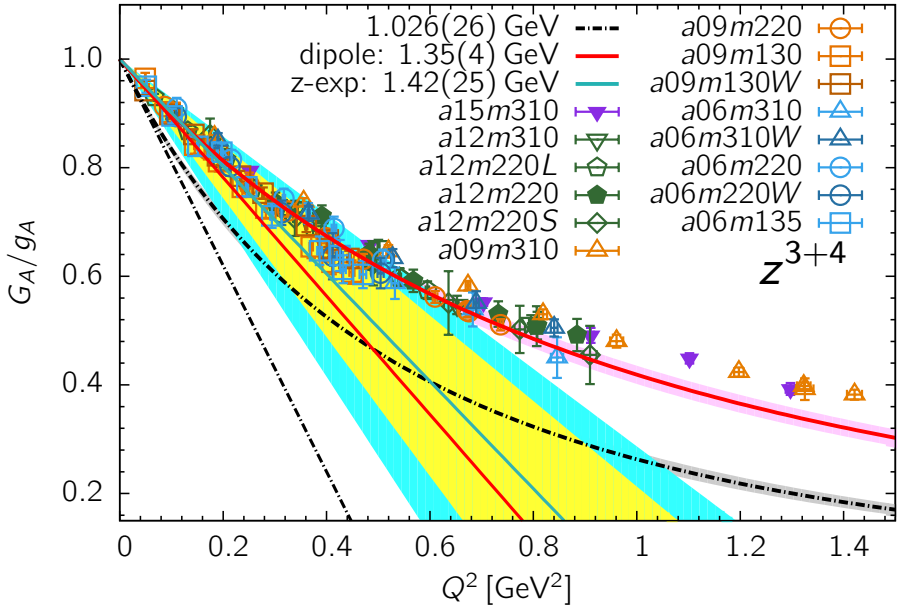

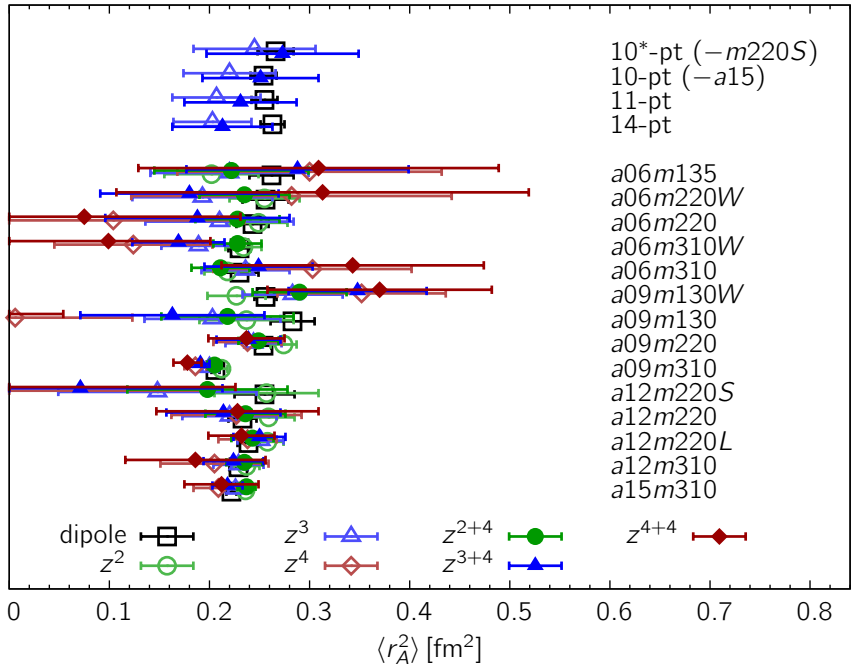

- 11-point extrapolation $\langle r_A^2 \rangle(a, M_\pi, M_\pi L)$
- $r_A = 0.481(58)(62)\,\mathrm{fm}$, $\mathcal{M}_A = 1.42(17)(18)\,\mathrm{GeV}$ from z-expansion fit @ z^{3+4}
- $r_A = 0.505(13)(6)\,\mathrm{fm}$, $\mathcal{M}_A = 1.35(3)(2)\,\mathrm{GeV}$ from dipole fit cf. $\mathcal{M}_A = 1.35(17)\mathrm{GeV}$ (MiniBooNE)
- systematic error: difference of $\langle r_A^2 \rangle$ from two physical ensembles
- $r_A = 0.48(4)\mathrm{fm}$ (PNDME2017) [R. Gupta, *et. al.* Phys. Rev. D96 no.11, 114503 (2017)]
- $r_A = 0.666(17)\mathrm{fm}$, $\mathcal{M}_A = 1.026(26)\mathrm{GeV}$ (neutrino scattering)
- $r_A = 0.68(16)\mathrm{fm}$, $\mathcal{M}_A = 1.00(24)$ (Deuterium) [Phys. Rev. D93 ,113015 (2016)]

Axial Charge Radius $\langle r_A^2 \rangle$: dipole versus z^{3+4}

$$\langle r_A^2 \rangle = c_1^A + c_2^A a + c_3^A M_\pi^2 + c_4^A M_\pi^2 e^{-M_\pi L}$$

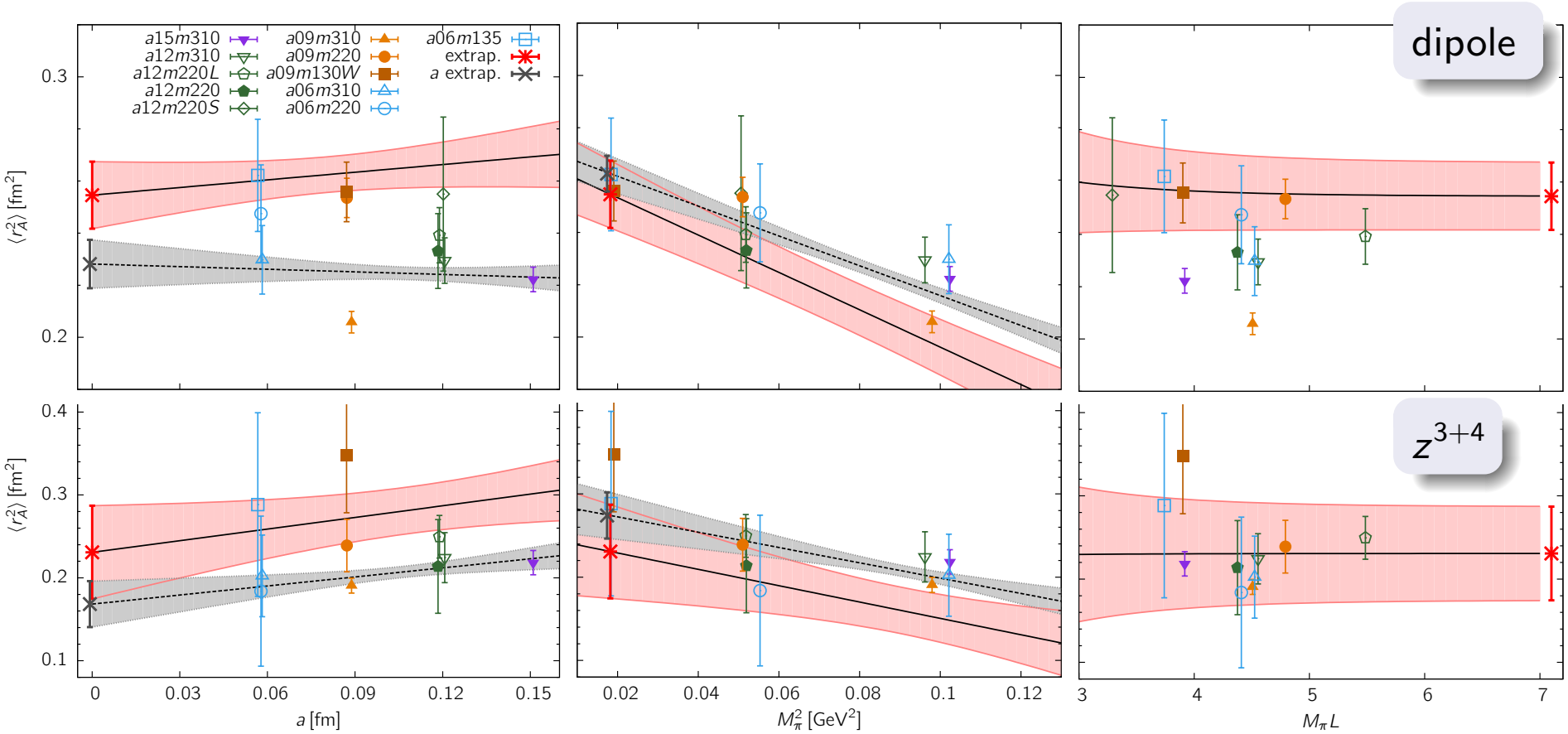

Summary

	r_E [fm]	r_M [fm]	μ	r_A [fm]	$\mathcal{M}_A$ [GeV]
z-exp.	0.804(42)(98)	0.736(166)(86)	3.99(32)(17)	0.481(58)(62)	1.42(17)(18)
dipole	0.772(10)(8)	0.722(23)(41)	3.96(10)(12)	0.505(13)(6)	1.35(3)(2)

- Dipole ansatz is surprisingly good.
- Estimates from dipole and z-expansion are consistent.
- Fits to G_M are the least stable.
- 'M_π' dependence is dominant in the continuum chiral extrapolation of $r_{E,M,A}$.
- 'a' dependence is dominant in the continuum chiral extrapolation of μ.

- r_E, r_M, μ are smaller than the phenomenology.
- $\mathcal{M}_A$ is consistent with the value 1.35(17) GeV used by miniBooNE to fit data
- $\mathcal{M}_A$ is larger than phenomenology:
  - 1.026(21) ($\nu, \bar{\nu}$ scattering) [dipole]
  - 1.069(16) (Electroproduction) [dipole]
  - 1.00(24) (Deuterium) [z-expansion]

- $\langle NA_\mu N \rangle$ and $\langle NPN \rangle$ satisfy the PCAC relation
- Three FFs G_A, $\widetilde{G}_P$, G_P extracted from them do not satisfy PCAC relation.
  $\rightarrow$ not resolved yet

Thank you for your attention.

Thanks for computing allocations to
NERSC, OLCF (TITAN), USQCD-Fermilab, and LANL